Check for updates

New global dynamical results and application of several SVEIS epidemic models with temporary immunity

Lianwen Wang[a], Zhijun Liu[a,*], Caihong Guo[b], Yong Li[c], Xinan Zhang[d]

[a] Department of Mathematics, Hubei Minzu University, Enshi 445000, P.R.China
[b] Enshi Special Care Hospital, Enshi 445000, P.R.China
[c] School of Information and Mathematics, Yangtze University, Jingzhou 434023, P.R.China
[d] School of Mathematics and Statistics, Central China Normal University, Wuhan 430079, P.R.China

ARTICLE INFO

ABSTRACT

This work applies a novel geometric criterion for global stability of nonlinear autonomous differential equations generalized by Lu and Lu (2017) to establish global threshold dynamics for several SVEIS epidemic models with temporary immunity, incorporating saturated incidence and nonmonotone incidence with psychological effect, and an SVEIS model with saturated incidence and partial temporary immunity. Incidentally, global stability for the SVEIS models with saturated incidence in Cai and Li (2009), Sahu and Dhar (2012) is completely solved. Furthermore, employing the DEDiscover simulation tool, the parameters in Sahu and Dhar'model are estimated with the 2009–2010 pandemic H1N1 case data in Hong Kong China, and it is validated that the vaccination programme indeed avoided subsequent potential outbreak waves of the pandemic. Finally, global sensitivity analysis reveals that multiple control measures should be utilized jointly to cut down the peak of the waves dramatically and delay the arrival of the second wave, thereinto timely vaccination is particularly effective.

1. Introduction

Immunization is believed to be one of the most successful and cost-effective public health interventions [1], for instance in worldwide eradication of small-pox and sharp reduction in the annual morbidity of most other vaccine-preventable diseases, such as polio, measles, hepatitis B, yellow fever [2], cholera [3], mumps [4] and influenza [5–8]. Currently, immunization saves 2–3 million lives yearly and prevents debilitating illness, disability and death from the diseases. However, it is estimated that 19.4 million infants failed to be reached with routine immunization services in 2018 [1]. Due to low vaccination rate, the 2017–2018 seasonal influenza caused estimated 45 million illnesses, 21 million medical visits, 810,000 hospitalizations and 61,000 deaths in the United States [9], and now burden is not optimistic. Fortunately, timely vaccination programme played a core part in mitigating the pandemic (H1N1) 2009 [8] (pH1N1). Take Hong Kong China for instance: the subsequent potential waves of the pandemic [10] might be effectively mitigated with the launch of the pH1N1 vaccination programme for several priority groups [11], although the first wave failed to be timely contained due to the unavailability of the vaccine against the novel influenza strain [12] (see Fig. 1).

---

* Corresponding author.
E-mail addresses: wanglianwen1987@hotmail.com (L. Wang), zhijun_liu47@hotmail.com (Z. Liu), guocaihong1988@hotmail.com (C. Guo), yongli@yangtzeu.edu.cn (Y. Li), zhangxinan@hotmail.com (X. Zhang).
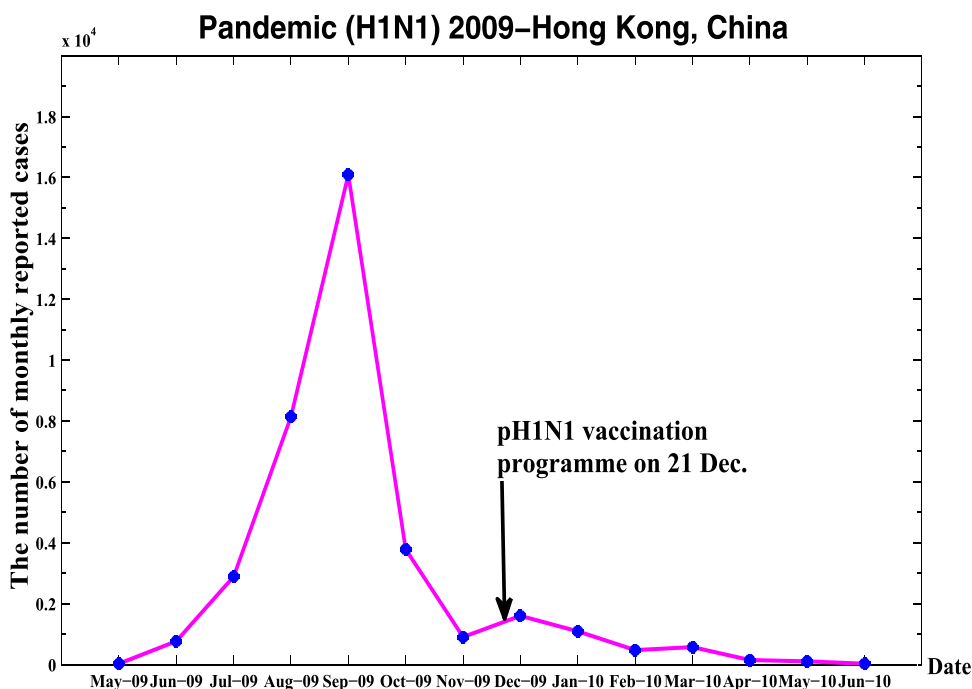
Fig. 1. Epidemic curve of the reported pH1N1 cases in Hong Kong China, 2009–2010.

Admittedly, immunization may not be once and for all because vaccine-induced immunity is generally temporary, and so are disease-acquired and natural immunity, which becomes one of major obstacles eliminating such these infectious diseases. Vaccines rarely provide the recipients with almost life-long immunity against re-infection. After being infected, susceptible individuals first become exposed but not infectious and then become infectious. The successfully recovered individuals acquire disease-induced immunity. Additionally, by virtue of natural immunity [13–15], a part of exposed individuals fail to develop disease but acquire temporary immunity. For example, the efficient innate immunity protects more than 90% of individuals infected with *Mycobacterium tuberculosis* [14]. A recent study [15] has showed that, similar to seasonal influenza, most infection (up to 75%) of the pandemic H1N1 strain was asymptomatic and gave the infected individuals temporary immunity.

The nonlinear epidemic dynamical models incorporating both temporary immunity and latency such as SEIRS, SVEIS models in [16–19], have been developed to better understand the transmission dynamical behaviors of infectious diseases qualitatively and quantitatively. The exploitation of their global asymptotic stability has been of great interest and challenging to researchers in infectious disease modelling aimed at finding out the effective control interventions, seeing [16–19]. While the Lyapunov function methods may become unsuitable to prove their global stability, the classical geometric approach for nonlinear autonomous differential equations based on additive compound matrix theory developed by Li and Muldowney [20–22] has been succeed in applying to these epidemic models [16,17,20–22]. For example, Cai and Li [16] proposed the following nonlinear SEIV epidemic model with temporary immunity:

$$
\begin{cases}
\dfrac{dS}{dt} = (1-p)\Pi - \dfrac{\beta SI}{\varphi(I)} - \mu S + \omega V, \\[2mm]
\dfrac{dE}{dt} = \dfrac{\beta SI}{\varphi(I)} - (\mu + \sigma)E, \\[2mm]
\dfrac{dI}{dt} = \sigma E - (\mu + \gamma)I, \\[2mm]
\dfrac{dV}{dt} = p\Pi + \gamma I - (\mu + \omega)V,
\end{cases}
\tag{1.1}
$$

where the total population N consists of susceptible (S), latent (E), infectious (I) and vaccinated-recovered (V) classes. The nonlinear incidence $\beta SI/\varphi(I)$, with $\varphi(0) = 1$ and $\varphi'(I) \geq 0$, generalizes saturated incidence $\beta SI/(1+\kappa I)$ and nonmonotone incidence capturing psychological effect $\beta SI/(1+\kappa I^2)$ [23,24]. Along the work of [16], Sahu and Dhar [17] further developed

Table 1
Notation description for model (1.2) and their values.

Notation	Description	Units	Range	Baseline	Source
Π	Recruitment rate	m^{-1}	[0,6748]	130	Assumed
μ	Natural death rate	m^{-1}	–	9.815×10^{-4}	[25]
$1/\gamma$	The mean infectious period	m	[0.1333,0.3333]	0.2333	[5,26–28]
$1/\omega$	Average time of immunity waning	m	[6,12.1655]	12.1655	[6,7]
α	Vaccination rate	m^{-1}	[0,1]	0	[5,7]
ξ	The recovery rate of exposed class due to natural immunity	m^{-1}	[3,30]	4.2857	fitted
β	The disease transmission coefficient	m$^{-1} \cdot p^{-1}$	[0,1]	7.0219×10^{-5}	Fitted
$1/\sigma$	The latent period	m	[0.0333,0.1667]	0.1116	Fitted
κ	The inhibition effect	–	[0,1]	1.3458×10^{-13}	Fitted
q	Fraction of recovered individuals from disease developing immunity	–	[0,1]	0.9287	Fitted
$S(0)$	Initial value for susceptible class	p	[0, 7×10^6]	1.2959×10^5	Fitted
$V(0)$	Initial value for vaccinated class	p	[0, 7×10^6]	2.7970×10^5	Fitted
$E(0)$	Initial value for exposed class	p	[0, 7×10^6]	10	Assumed
$I(0)$	Initial value for infectious class	p	–	23	[12]

[Note: m, p represent month and person, respectively.]

a nonlinear SVEIS model with partial temporary immunity as follows:

$$\begin{cases} \dfrac{dS}{dt} = \Pi - \alpha S - \dfrac{\beta SI}{1+\kappa I} - \mu S + \omega V + (1-q)\gamma I, \\[2mm] \dfrac{dV}{dt} = \alpha S + q\gamma I + \xi E - (\mu+\omega)V, \\[2mm] \dfrac{dE}{dt} = \dfrac{\beta SI}{1+\kappa I} - (\mu+\sigma+\xi)E, \\[2mm] \dfrac{dI}{dt} = \sigma E - (\mu+\gamma)I, \end{cases} \qquad (1.2)$$

where susceptible class are vaccinated with certain vaccine at constant rate α, different from model (1.1) with a fraction of vaccinated newborns (denoted by p). We always assume that the same parameter represents the identical biological meaning throughout this paper, and the detailed biological descriptions of the parameters for model (1.2) are demonstrated in Table 1. Note that [16,17] applied the geometric approach based on the second additive compound matrix theory of [20] to the responding limiting systems and achieved global stability of the unique endemic equilibrium (EE) under the vaccination reproduction number $\mathfrak{R}_v > 1$ and some additional restrictions. More recently, Lu and Lu [18,19] improved the classical geometric approach of [20–22] and generalized the geometric criterion on global-stability problem and applied it to several nonlinear SEIRS models, successfully removing some restrict conditions on global stability of their EE.

Borrowing the ideas of [16,17,23,24], we establish the following SVEIS epidemic model with general nonlinear incidence:

$$\begin{cases} \dfrac{dS}{dt} = (1-p)\Pi - Sg(I) - \mu S + \omega V, \\[2mm] \dfrac{dV}{dt} = p\Pi + \gamma I + \xi E - (\mu+\omega)V, \\[2mm] \dfrac{dE}{dt} = Sg(I) - (\mu+\sigma+\xi)E, \\[2mm] \dfrac{dI}{dt} = \sigma E - (\mu+\gamma)I, \end{cases} \qquad (1.3)$$

in which, it is assumed that vaccine-induced, disease-acquired and natural immunity may last the nearly same time for some diseases like influenza, and the differential infectious force function g possesses the following properties reflecting some biological significances:

(P1) $g \in \mathbb{C} : \mathbb{R}_+ \to \mathbb{R}_+$, satisfies $g(0) = 0$, $g(I) > 0$ for $I > 0$.
(P2) $g(I)/I \in \mathbb{C}$ is monotonously nonincreasing for $I > 0$, and $\lim_{I \to 0^+} (g(I)/I) := \beta < +\infty$.
(P3) $I|g'(I)| \leq g(I)$ for $I > 0$.

It is worth highlighting that saturated and nonmonotone incidences in [23,24], $\beta S \ln(1+\kappa I)$ [29] and $\beta SI/(1+\kappa I + \sqrt{1+2\kappa I})$ [30], but not confined to them, fulfill **(P1)-(P3)**, thus we lift restrictions on monotonicity of $g(I)$ in spite of the introduction of **(P3)**. With this geometric criterion in [18], we shall thoroughly address global threshold dynamics of models (1.3) and (1.2), characterized by their vaccination reproduction numbers. Incidentally, the unnecessary restrictions both in
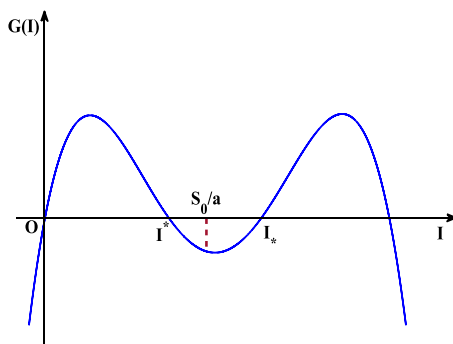
Fig. 2. The existence and uniqueness of positive real root for Eq. (2.2).

Theorem 4 in [16] and Theorem 5.5 in [17] are completely removed since model (1.3) reduces to model (1.1) if $g(I) = \beta I/\varphi(I)$ and $\xi = 0$. Of particular note is that we achieve global asymptotic stability for model (1.1) of [16] with nonmonotone incidence reflecting psychological effect, which also reserves threshold dynamics.

Furthermore, as an application of model (1.2), the reported pH1N1 case data of Hong Kong China [12] are utilized to estimate its parameters, aimed at accounting for the avoidance of the subsequent potential waves of the pandemic in 2010 (as predicted by WHO [10]) with the pH1N1 vaccination programme. Meanwhile, several disease-control measures are evaluated in terms of global sensitivity analysis for the vaccination reproduction number. In particular, this study arrives at a conclusion that joint usage of multiple control measures such as isolation, vaccination and treatment, can more effectively cut down the peak of the waves and dramatically delay the arrival of the second wave at the same time.

The outline of this paper is summarized as follows. In Section 2, we offer insight into global threshold dynamics for model (1.3), including the existence, local and global asymptotic stability of its equilibria. Section 3 completely addresses the global dynamics of model (1.2). Section 4 performs parameter estimation and global sensitivity analysis for the vaccination reproduction number of model (1.2) with the purpose of seeking for effective control measures. Finally, we close the paper with a conclusion and discussion section.

2. Global threshold dynamics for model (1.3)

2.1. The existence of the equilibria

For model (1.3), one can easily obtain that the biologically feasible region

$$\Omega = \left\{ (S, V, E, I) \in \mathbb{R}_+^4 : N = S + V + E + I \leq \frac{\Pi}{\mu} \right\},$$

is the positively invariant set by similar arguments in [16]. Apparently, the disease-free equilibrium (DFE) $P_0 = (S_0, V_0, 0, 0)$ of model (1.3) always exists, where $S_0 = [(1 - p)\mu + \omega]\Pi/[\mu(\mu + \omega)]$, $V_0 = p\Pi/(\mu + \omega)$. Thus, by application of the next generation matrix approach in [31], the vaccination reproduction number (e.g., seeing [32,33]) is calculated as

$$\mathfrak{R}_v = \frac{\sigma g'(0)S_0}{(\mu + \gamma)(\mu + \sigma + \xi)} = \frac{\sigma \beta \Pi[(1 - p)\mu + \omega]}{\mu(\mu + \omega)(\mu + \gamma)(\mu + \sigma + \xi)}, \tag{2.1}$$

clearly remaining the same with the model in [16] when $\xi = 0$.

By some direct but tedious algebra operations, it can be deduced that the I^* component in the EE $P^* = (S^*, V^*, E^*, I^*)$ is determined by the following equation

$$G(I) := (S_0 - aI)g(I) - bI = 0, \quad \text{for} \quad I \in [0, S_0/a], \tag{2.2}$$

where

$$a := \frac{(\mu + \gamma)(\mu + \sigma + \xi + \omega) + \sigma \omega}{\sigma(\mu + \omega)}, \quad b := \frac{(\mu + \gamma)(\mu + \sigma + \xi)}{\sigma}.$$

In what follows, we are going to focus mainly on analyzing the positive real solution of Eq. (2.2). A simple induction then shows

$$G'(I) := (S_0 - aI)g'(I) - ag(I) - b. \tag{2.3}$$

It deduces from **(P2)** that $G'(0) = S_0 g'(0) - b = b(\mathfrak{R}_v - 1)$.

In the case of $\mathfrak{R}_v > 1$, together with $G'(0) > 0$, $G(0) = 0$ and $G(S_0/a) = -bS_0/a < 0$, it can be revealed that $G(I) > 0$ as I is sufficiently small, guaranteeing the existence of positive real root for Eq. (2.2) from Fig. 2, denoted by I^*. And its uniqueness is verified by reduction to absurdity as follows. Provided that another positive solution I_* of (2.2) nearest to I^*, if it exists,

must satisfy $G'(I_*) \geq 0$ owing to the continuity of $G(I)$. Actually, together with $g'(I_*) \leq g(I_*)/I_*$ deduced from **(P3)**, we arrive at

$$G'(I_*) := S_*g'(I_*) - ag(I_*) - \frac{S_*g(I_*)}{I_*} = -ag(I_*) + S_*\left(g'(I_*) - \frac{g(I_*)}{I_*}\right) < 0, \tag{2.4}$$

where one utilizes the equality $b = S_*g(I_*)/I_*$ derived by the equations that the EE satisfies. An obvious contradiction exists as shown in Fig. 2. Thus, the positive solution I^* is unique, which can lead to the uniqueness of S^*, V^*, E^* from the analysis above.

In the case of $\Re_v \leq 1$, Eq. (2.2) must admit no positive solution. Otherwise, let $I_\star$ be its smallest one. Combining $G(0) = 0$ and $G'(0) \leq 0$ yields that $G(I) \leq 0$ for sufficiently small I. Since the function $G(I)$ continuously increases to 0 from the non-positive value, it is clear to see that $G'(I_\star) \geq 0$, which contradicts with $G'(I_\star) < 0$ in (2.4).

To sum up, model (1.3) has a unique EE P^* if and only if (iff) $\Re_v > 1$.

Theorem 2.1. *For model (1.3), a DFE P_0 always exists and the EE P^* exists uniquely iff $\Re_v > 1$.*

2.2. Local stability

Theorem 2.2. (i) *The DFE P_0 is local asymptotically stable (LAS) if $\Re_v < 1$, but becomes unstable if $\Re_v > 1$; (ii) The EE P^* is LAS iff $\Re_v > 1$.*

Proof. The Jacobian matrix of model (1.3) takes the following form of

$$\mathcal{J} = \begin{bmatrix} -(\mu + g(I)) & \omega & 0 & -Sg'(I) \\ 0 & -(\mu + \omega) & \xi & \gamma \\ g(I) & 0 & -(\mu + \sigma + \xi) & Sg'(I) \\ 0 & 0 & \sigma & -(\mu + \gamma) \end{bmatrix}. \tag{2.5}$$

(i) The characteristic equation at P_0 is

$$(\lambda + \mu)(\lambda + \mu + \omega)[\lambda^2 + (2\mu + \gamma + \sigma + \xi)\lambda + (\mu + \gamma)(\mu + \sigma + \xi)(1 - \Re_v)] = 0. \tag{2.6}$$

Obviously, its all eigenvalues possess negative real parts when $\Re_v < 1$, that is, P_0 is LAS. If $\Re_v > 1$, there exists a positive root, so the DFE becomes unstable.

(ii) Calculating the characteristic equation at P^*, one reaches

$$(\lambda + \mu)[(\lambda + a_1)(\lambda + a_2)(\lambda + a_3) + \omega g(I^*)(\lambda + a_4) - \sigma S^*g'(I^*)(\lambda + a_5)] = 0, \tag{2.7}$$

where $a_1 := \mu + \gamma$, $a_2 := \mu + \sigma + \xi$, $a_3 := \mu + \omega + g(I^*)$, $a_4 := \mu + \gamma + \sigma$, $a_5 := \mu + \omega$. Clearly, $\lambda_1 = -\mu < 0$.

Case I. Let $g'(I^*) > 0$. One asserts that all eigenvalues of the following equation

$$(\lambda + a_1)(\lambda + a_2)(\lambda + a_3) + \omega g(I^*)(\lambda + a_4) = \sigma S^*g'(I^*)(\lambda + a_5) \tag{2.8}$$

satisfy $Re\lambda < 0$. Suppose, for contradiction, that there exists one eigenvalue $\tilde{\lambda}$ with $Re\tilde{\lambda} \geq 0$. From (2.8) and **(P3)**, the following contradiction is attained

$$a_1a_2 < \left|(\tilde{\lambda} + a_1)(\tilde{\lambda} + a_2)\left(1 + \frac{g(I^*)}{\tilde{\lambda} + a_5}\right) + \frac{\omega g(I^*)(\tilde{\lambda} + a_4)}{\tilde{\lambda} + a_5}\right| = \sigma S^*g'(I^*) \leq \frac{\sigma S^*g(I^*)}{I^*} = a_1a_2.$$

Case II. Let $g'(I^*) \leq 0$. Equality (2.8) is recast as $\lambda^3 + A_1\lambda^2 + A_2\lambda + A_3 = 0$. For $i, j = 1, 2, 3$, the Routh-Hurwitz conditions can be ensured by

$$A_1 = a_1 + a_2 + a_3 > 0,$$
$$A_2 = a_1a_2 + a_2a_3 + a_1a_3 + \omega g(I^*) - \sigma S^*g'(I^*) > 0,$$
$$A_3 = a_1a_2a_3 + \omega g(I^*)a_4 - \sigma S^*g'(I^*)a_5 > 0,$$
$$A_1A_2 - A_3 = (a_1 + a_2 + a_3)(a_1a_2 + a_2a_3 + a_1a_3) - a_1a_2a_3 + \omega g(I^*)(2\mu + \xi + \omega + g(I^*)) - \sigma S^*g'(I^*)(a_1 + a_2 + g(I^*)) > 0.$$

We thus infer that all eigenvalues obey $Re\lambda < 0$. Combining *Cases I* and *II* leads to local stability of P^* for $\Re_v > 1$. $\square$

2.3. Global stability

Theorem 2.3. *The DFE P_0 of model (1.3) is GAS in Ω if $\Re_v \leq 1$.*

Proof. By the first equation of (1.3) and $S + V + E + I \leq \Pi/\mu$, it is easy to ascertain that

$$\frac{dS}{dt} \leq (1-p)\Pi - \mu S + \omega V \leq (1-p)\Pi - \mu S + \omega\left(\frac{\Pi}{\mu} - S - E - I\right)$$

$$\leq \frac{[(1-p)\mu + \omega]\Pi}{\mu} - (\mu + \omega)S = (\mu + \omega)(S_0 - S),$$

which asserts that $S \leq S_0$ (similar to [4]). Otherwise, let us suppose that $S > S_0$, thus $dS/dt < 0$. It follows that $S \leq S_0$ when $S(0) \leq S_0$, which is absurd as our assumption. Hence, our claim $S \leq S_0$ is valid. Observe that $g(I)/I \leq \beta$ for $I > 0$ can be

ensured by **(P3)** (seeing, e.g., [34]). Construct Lyapunov function $\mathbf{W}(t) = E + (\mu + \sigma + \xi)I/\sigma$, and its time derivative of $\mathbf{W}(t)$ along the solutions of model (1.3) is estimated as

$$\frac{d\mathbf{W}(t)}{dt} = \frac{dE}{dt} + \frac{\mu + \sigma + \xi}{\sigma}\frac{dI}{dt} = I\left(S\frac{g(I)}{I} - b\right) \le I(\beta S_0 - b) = bI(\mathfrak{R}_\nu - 1) \le 0$$

provided that $\mathfrak{R}_\nu \le 1$. From the LaSalle's Invariance Principle [35] and local stability of P_0 in Theorem 2.2, we can derive its global asymptotic stability for $\mathfrak{R}_\nu \le 1$. $\square$

In the sequel, we shall employ the general criterion for global stability for autonomous differential equations developed by [18] to establish global stability of the EE P^* of model (1.3). A brief outline on this geometrical approach [18,20–22] is presented as follows.

Let us consider the nonlinear autonomous dynamical system:

$$\frac{dx}{dt} = f(x), x \in Q \subset \mathbb{R}^n, \tag{2.9}$$

where the function $f(x) \in \mathbb{C} : Q \to \mathbb{R}^n$ and Q is an open set. For (2.9), the solution with $x(0, x_0) = x_0$ is defined as $x(t, x_0)$ and its equilibrium as x^*. Moreover, let us assign $\mathcal{M}(x) \in \mathbb{C}^2 : Q \to \mathbb{R}^n$, satisfying $\dim(\partial \mathcal{M}/\partial x) = m$ when $\mathcal{M}(x) = 0$. We assume that system (2.9) admits a $n - m$ dimensional invariant manifold defined by $\Gamma = \{x \in \mathbb{R}^n | \mathcal{M}(x) = 0\}$.

The following three hypotheses are satisfied:

(H1) Γ is simply connected.
(H2) There is a compact absorbing set $D \subset Q \subset \Gamma$.
(H3) System (2.9) admits a unique equilibrium x^* in Γ.
The general geometric criterion of Lu and Lu is recapped as follows.

Lemma 2.1. *(see Theorem 2.6 in [18]). The unique equilibrium x^* of (2.9) is globally asymptotically stable (GAS) in Γ provided that **(H1)**-**(H3)** and the following condition **(C)** hold.*

(C) For the coefficient matrix $B(x(0, x_0))$ of system (2.9), there are a matrix $C(t)$, a sufficiently large $\tau_1 > 0$ and constants $\rho_1, \rho_2, \ldots, \rho_n > 0$ such that

$$b_{ii}(t) + \sum_{i \ne j} \frac{\rho_j}{\rho_i}|b_{ij}(t)| \le c_{ii}(t) + \frac{\rho_j}{\rho_i}|c_{ij}(t)|, \text{ for } \forall t \ge \tau_1, \quad \forall x_0 \in D, \tag{2.10}$$

and

$$\lim_{t \to \infty} \frac{1}{t}\int_0^t \left(c_{ii}(t) + \frac{\rho_j}{\rho_i}|c_{ij}(t)|\right)ds = \bar{c}_i < 0, \tag{2.11}$$

where $b_{ij}(t)$ and $c_{ij}(t)$ stand for entries of matrices $B(x(0, x_0))$ and $C(t)$, respectively.

Denote the interior, the boundary of Ω by $\mathring{\Omega}$ and $\partial\Omega$, respectively. Uniform persistence in $\mathring{\Omega}$ of model (1.3) for $\mathfrak{R}_\nu > 1$ can be deduced from the instability of P_0 and $P_0 \in \partial\Omega$.

Theorem 2.4. *Model (1.3) is uniform persistent in $\mathring{\Omega}$ if $\mathfrak{R}_\nu > 1$.*

Theorem 2.5. *The EE P^* of model (1.3) is GAS in $\mathring{\Omega}$ if $\mathfrak{R}_\nu > 1$.*

Proof. The third additive compound matrix of $\mathcal{J}$ [22] for model (1.3) acquires the form

$$\mathcal{J}^{[3]}(x) = \begin{bmatrix} -(\omega + \sigma + \xi) & Sg'(I) & -\gamma & -Sg'(I) \\ \sigma & -(\omega + \gamma) & \xi & 0 \\ 0 & 0 & -(\sigma + \xi + \gamma) & \omega \\ 0 & -g(I) & 0 & -(\omega + \sigma + \xi + \gamma) \end{bmatrix} + \Theta_1,$$

where $\Theta_1 := \text{diag}\{-(3\mu + g(I)), -(3\mu + g(I)), -(3\mu + g(I)), -3\mu\}$.

Assign $\mathbf{M}(\mathbf{x}) = S + V + E + I - \Pi/\mu$ with $\mathbf{x} = (S, V, E, I) \in \mathbb{R}^4_+$. The invariant manifold for (1.3) is $\Gamma = \{\mathbf{x} \in \mathbb{R}^4_+ | \mathcal{M}(\mathbf{x}) = 0\}$. Following [22], it turns out to be $\mathbf{N}(\mathbf{x}) = \nu(\mathbf{x}) = -\mu$ and $m = \dim(\partial\mathbf{M}/\partial\mathbf{x}) = 1$. In the sequel, let $P(x) = \text{diag}\{I, E, V, S\}$ and $\mathbb{I}_{4\times4}$ be the 4×4 identity matrix. Then the coefficient matrix $B(t) = P_f P^{-1} + P\mathcal{J}^{[3]}(x)P^{-1} - \nu\mathbb{I}_{4\times4}$ reads

$$B(t) = \begin{bmatrix} -(\omega + \sigma + \xi) & \dfrac{SIg'(I)}{E} & -\dfrac{\gamma I}{V} & -Ig'(I) \\ \dfrac{\sigma E}{I} & -(\omega + \gamma) & \dfrac{\xi E}{V} & 0 \\ 0 & 0 & -(\sigma + \xi + \gamma) & \dfrac{\omega V}{S} \\ 0 & -\dfrac{Sg(I)}{E} & 0 & -(\omega + \sigma + \xi + \gamma) \end{bmatrix} + \Theta_2,$$

where $\Theta_2 = \text{diag}\{-(2\mu + g(I)) + I'/I, -(2\mu + g(I)) + E'/E, -(2\mu + g(I)) + V'/V, -2\mu + S'/S\}$.

Meanwhile, model (1.3) can be recast into

$$
\frac{\omega V}{S} = \frac{S^{'}}{S} + g(I) + \mu - \frac{(1-p)\Pi}{S}, \quad \frac{\gamma I}{V} = \frac{V^{'}}{V} + \mu + \omega - \frac{p\Pi}{V} - \frac{\xi E}{V},
$$
$$
\frac{Sg(I)}{E} = \frac{E^{'}}{E} + \mu + \sigma + \xi, \frac{\sigma E}{I} = \frac{I^{'}}{I} + \mu + \gamma. \tag{2.12}
$$

Note that Theorem 2.4 implies that there is a constant $\pi_0 > 0$ such that $\pi_0 \leq S, V, E, I \leq \Pi/\mu$. It follows from **(P1)** that there are constants $l, L > 0$ such that $l \leq g(I) \leq L$. Assign $\pi := \mu\pi_0/\Pi$. By $I|g^{'}(I)| \leq g(I)$ in **(P3)** and (2.12), $c_i(t)$ are respectively estimated as

$$
c_1(t) = b_{11}(t) + \sum_{i=2}^{4}\left|b_{ij}(t)\right| = -(2\mu + \omega + \sigma + \xi + g(I)) + \frac{I^{'}}{I} + \frac{SI|g^{'}(I)|}{E} + \frac{\gamma I}{V} + I|g^{'}(I)|
$$

$$
\leq -(2\mu + \omega + \sigma + \xi + g(I)) + \frac{I^{'}}{I} + \frac{Sg(I)}{E} + \frac{\gamma I}{V} + g(I)
$$

$$
\leq -(2\mu + \omega + \sigma + \xi + g(I)) + \frac{I^{'}}{I} + \left(\frac{E^{'}}{E} + \mu + \sigma + \xi\right)
$$

$$
+ \left(\frac{V^{'}}{V} + \mu + \omega - \frac{p\Pi}{V} - \frac{\xi E}{V}\right) + g(I)
$$

$$
\leq \frac{V^{'}}{V} + \frac{E^{'}}{E} + \frac{I^{'}}{I} - (p\mu + \xi\pi) \triangleq \bar{c}_1(t),
$$

$$
c_2(t) = b_{22}(t) + \sum_{i\neq 2}\left|b_{ij}(t)\right| = -(2\mu + \omega + \gamma + g(I)) + \frac{E^{'}}{E} + \frac{\sigma E}{I} + \frac{\xi E}{V}
$$

$$
\leq -(2\mu + \omega + \gamma + g(I)) + \frac{E^{'}}{E} + \left(\frac{I^{'}}{I} + \mu + \gamma\right) + \left(\frac{V^{'}}{V} + \mu + \omega - \frac{p\Pi}{V} - \frac{\gamma I}{V}\right)
$$

$$
\leq \frac{V^{'}}{V} + \frac{E^{'}}{E} + \frac{I^{'}}{I} - (l + p\mu + \gamma\pi) \triangleq \bar{c}_2(t),
$$

$$
c_3(t) = b_{33}(t) + \sum_{i\neq 3}\left|b_{ij}(t)\right| = -(2\mu + \sigma + \gamma + \xi + g(I)) + \frac{V^{'}}{V} + \frac{\omega V}{S}
$$

$$
\leq -(2\mu + \sigma + \gamma + \xi + g(I)) + \frac{V^{'}}{V} + \left(\frac{S^{'}}{S} + g(I) + \mu - \frac{(1-p)\Pi}{S}\right)
$$

$$
\leq \frac{S^{'}}{S} + \frac{V^{'}}{V} - [\sigma + \gamma + \xi + (2-p)\mu] \triangleq \bar{c}_3(t),
$$

$$
c_4(t) = b_{44}(t) + \sum_{i\neq 4}\left|b_{ij}(t)\right| = -(2\mu + \sigma + \gamma + \omega + \xi) + \frac{S^{'}}{S} + \frac{Sg(I)}{E}
$$

$$
\leq -(2\mu + \sigma + \gamma + \omega + \xi) + \frac{S^{'}}{S} + \left(\frac{E^{'}}{E} + \mu + \sigma + \xi\right)
$$

$$
\leq \frac{S^{'}}{S} + \frac{E^{'}}{E} - (\mu + \omega + \gamma) \triangleq \bar{c}_4(t).
$$

Choose the matrix $C(t)$ in Lemma 2.1 as $C(t) = diag\{c_1(t), c_2(t), c_3(t), c_4(t)\}$. It is easy to check that $\lim_{t\to\infty}\int_0^t \bar{c}_i(s)ds/t = \bar{c}_i < 0$, where $\bar{c}_1 = -(p\mu + \xi\pi)$, $\bar{c}_2 = -(l + p\mu + \gamma\pi)$, $\bar{c}_3 = -[\sigma + \gamma + \xi + (2-p)\mu]$, $\bar{c}_4 = -(\mu + \omega + \gamma)$. By Lemma 2.1, the EE is GAS in $\mathring{\Omega}$. □

Remark 2.1. Let $\xi = 0$ and $g(I) = \beta I/(1+\kappa I)$, then model (1.3) reduces to the model with saturated incidence of [16], which retains global threshold dynamics from Theorem 2.5, improving Theorem 4 in [16]. More importantly, the sharp threshold dynamics result is extended to the model with nonmonotone incidence capturing psychological effect of [16].

3. Global threshold dynamics for model (1.2)

In this section, for simplicity, we take $g(I) := \beta I/(1+\kappa I)$, satisfying **(P1), (P2)** and
(P3)′ $Ig^{'}(I) \leq g(I)$ for $I > 0$.
Following the same reasoning as the proof of Theorems 2.1–2.2 in Subsections 2.1–2.2, one easily draws the following conclusions on the existence, local stability of the DFE $\tilde{P}_0 = (\tilde{S}_0, \tilde{V}_0, 0, 0)$ and the EE $\tilde{P}^* = (\tilde{S}^*, \tilde{V}^*, \tilde{E}^*, \tilde{I}^*)$ for model (1.2), where $\tilde{S}_0 = (\mu + \omega)\Pi/[\mu(\mu + \alpha + \omega)]$, $\tilde{V}_0 = \alpha\Pi/[\mu(\mu + \alpha + \omega)]$.

Theorem 3.1. *Model (1.2) always has a DFE $\tilde{P}_0$ and the EE $\tilde{P}^*$ is unique if the vaccination reproduction number*

$$\tilde{\mathfrak{R}}_v = \frac{\sigma g'(0)\tilde{S}_0}{(\mu+\gamma)(\mu+\sigma+\xi)} = \frac{\sigma \beta \Pi (\mu+\omega)}{\mu(\mu+\alpha+\omega)(\mu+\gamma)(\mu+\sigma+\xi)} > 1. \tag{3.1}$$

Theorem 3.2. *The DFE $\tilde{P}_0$ is LAS when $\tilde{\mathfrak{R}}_v \leq 1$, and it is unstable but the EE $\tilde{P}^*$ is LAS when $\tilde{\mathfrak{R}}_v > 1$.*

In what follows, we make a thorough inquiry into global stability of model (1.2). Using the similar arguments as the analysis of Theorems 2.3-2.4 in Subsection 2.3 can lead to global stability of the DFE and persistence of model (1.2) as follows.

Theorem 3.3. *If $\tilde{\mathfrak{R}}_v \leq 1$, the DFE $\tilde{P}_0$ is GAS in Ω.*

Theorem 3.4. *If $\tilde{\mathfrak{R}}_v > 1$, model (1.2) is uniform persistent in $\mathring{\Omega}$.*

In order to achieve global stability of the EE, we focus mainly on the significant differences and skip the repeated parts with the proof of Theorem 2.3 in Subsection 2.3. The coefficient matrix $B(t)$ for model (1.2) is calculated as

$$B(t) = \begin{bmatrix} -(\alpha+\omega+\sigma+\xi) & \dfrac{SIg'(I)}{E} & -\dfrac{q\gamma I}{V} & -Ig'(I) + \dfrac{(1-q)\gamma I}{S} \\ \dfrac{\sigma E}{I} & -(\alpha+\omega+\gamma) & \dfrac{\xi E}{V} & 0 \\ 0 & 0 & -(\alpha+\sigma+\xi+\gamma) & \dfrac{\omega V}{S} \\ 0 & -\dfrac{Sg(I)}{E} & \dfrac{\alpha S}{V} & -(\omega+\sigma+\xi+\gamma) \end{bmatrix} + \tilde{\Theta}_2,$$

where $\tilde{\Theta}_2 = \text{diag}\{-(2\mu+g(I))+I'/I, -(2\mu+g(I))+E'/E, -(2\mu+g(I))+V'/V, -2\mu+S'/S\}$. And model (1.2) can be transformed into

$$\frac{\omega V}{S} = \frac{S'}{S} + g(I) + \mu + \alpha - \frac{\Pi}{S} - \frac{(1-q)\gamma I}{S}, \quad \frac{q\gamma I}{V} = \frac{V'}{V} + \mu + \omega - \frac{\alpha S}{V} - \frac{\xi E}{V},$$
$$\frac{Sg(I)}{E} = \frac{E'}{E} + \mu + \sigma + \xi, \quad \frac{\sigma E}{I} = \frac{I'}{I} + \mu + \gamma. \tag{3.2}$$

Clearly, $g(I)$ meets **(P1)**, **(P2)** and **(P3)′**, and $g'(I) > 0$ for $I > 0$. Uniform persistence ensures that there exists positive constants π_0, l, L such that $\pi_0 \leq S, V, E, I \leq \Pi/\mu$, and $l \leq g(I) \leq L$. Let $\pi := \mu\pi_0/\Pi$. Two cases will be considered to estimate $c_1(t)$.

Case 1. $g'(I) - (1-q)\gamma/S \geq 0$. Employing (3.2), $g'(I) > 0$ and **(P3)′** results in

$$c_1(t) = -(2\mu+\alpha+\omega+\sigma+\xi+g(I)) + \frac{I'}{I} + \frac{SI|g'(I)|}{E} + \frac{q\gamma I}{V} + \left| Ig'(I) - \frac{(1-q)\gamma I}{S} \right|$$

$$\leq -(2\mu+\alpha+\omega+\sigma+\xi+g(I)) + \frac{I'}{I} + \left(\frac{E'}{E} + \mu + \sigma + \xi \right) + \left(\frac{V'}{V} + \mu + \omega - \frac{\alpha S}{V} - \frac{\xi E}{V} \right) + g(I)$$

$$\leq \frac{V'}{V} + \frac{E'}{E} + \frac{I'}{I} - (\alpha + \alpha\pi + \xi\pi) \triangleq \bar{c}_1(t).$$

Case 2. $g'(I) - (1-q)\gamma/S < 0$. Similar proof in Theorem 2.3 gives $S \leq S_0$, being equivalent to $\mu+\alpha-\Pi/S \leq \alpha\omega/(\mu+\omega)$. By $g'(I) > 0$, we can arrive at

$$c_1(t) \leq -(2\mu+\alpha+\omega+\sigma+\xi+g(I)) + \frac{I'}{I} + \frac{Sg(I)}{E} + \frac{q\gamma I}{V} + \frac{(1-q)\gamma I}{S} - Ig'(I)$$

$$\leq -(2\mu+\alpha+\omega+\sigma+\xi+g(I)) + \frac{I'}{I} + \left(\frac{E'}{E} + \mu + \sigma + \xi \right)$$

$$+ \left(\frac{V'}{V} + \mu + \omega - \frac{\alpha S}{V} - \frac{\xi E}{V} \right) + \left(\frac{S'}{S} + g(I) + \mu + \alpha - \frac{\Pi}{S} - \frac{\omega V}{S} \right)$$

$$\leq \frac{S'}{S} + \frac{V'}{V} + \frac{E'}{E} + \frac{I'}{I} - \left(\frac{\mu\alpha}{\mu+\omega} + (\alpha+\xi+\omega)\pi \right) \triangleq \bar{c}_1(t).$$

We can similarly infer that

$$c_2(t) = -(2\mu+\alpha+\omega+\gamma+g(I)) + \frac{E'}{E} + \frac{\sigma E}{I} + \frac{\xi E}{V}$$

$$= -(2\mu+\alpha+\omega+\gamma+g(I)) + \frac{E'}{E} + \left(\frac{I'}{I} + \mu + \gamma \right) + \left(\frac{V'}{V} + \mu + \omega - \frac{\alpha S}{V} - \frac{q\gamma I}{V} \right)$$

$$\leq \frac{V^{`}}{V} + \frac{E^{`}}{E} + \frac{I^{`}}{I} - (\alpha + \alpha\pi + q\gamma\pi) \triangleq \overline{c}_2(t),$$

$$c_3(t) = -(2\mu + \alpha + \sigma + \gamma + \xi + g(I)) + \frac{V^{`}}{V} + \frac{\omega V}{S}$$

$$= -(2\mu + \alpha + \sigma + \gamma + \xi + g(I)) + \frac{V^{`}}{V} + \left( \frac{S^{`}}{S} + g(I) + \mu + \alpha - \frac{\Pi}{S} - \frac{(1-q)\gamma I}{S} \right)$$

$$\leq \frac{S^{`}}{S} + \frac{V^{`}}{V} - \left(2\mu + \sigma + \gamma + \xi + (1-q)\gamma\pi + \frac{\mu\alpha}{\mu+\omega} \right) \triangleq \overline{c}_3(t),$$

$$c_4(t) = -(2\mu + \sigma + \gamma + \omega + \xi) + \frac{S^{`}}{S} + \frac{\alpha S}{V} + \frac{Sg(I)}{E}$$

$$= -(2\mu + \sigma + \gamma + \omega + \xi) + \frac{S^{`}}{S} + \left( \frac{V^{`}}{V} + \mu + \omega - \frac{q\gamma I}{V} - \frac{\xi E}{V} \right) + \left(\frac{E^{`}}{E} + \mu + \sigma + \xi \right)$$

$$\leq \frac{S^{`}}{S} + \frac{V^{`}}{V} + \frac{E^{`}}{E} - (\gamma + q\gamma\pi + \xi\pi) \triangleq \overline{c}_4(t).$$

By applying Lemma 2.1, the above is concisely stated into Theorem 3.5.

Theorem 3.5. *The EE $\tilde{P}^*$ of model (1.2) is GAS in $\mathring{\tilde{\Omega}}$ if $\tilde{\mathfrak{R}}_v > 1$.*

Remark 3.1. An immediate consequence of Theorem 3.5 yields global threshold dynamics of model (1.2), getting rid of the unnecessary restrictions in Theorem 5.5 from [17]. Additionally, model (1.2) with the incidence satisfying **(P1)**,**(P2)** and **(P3)′**, e.g., $\beta S \ln(1 + \kappa I)$ [29], $\beta SI/(1 + \kappa I + \sqrt{1 + 2\kappa I})$ [30], also reserves global threshold stability by the same proof.

Remark 3.2. From the analysis in Sections 2 and 3, it can be similarly verified that the following SVEIS model with temporary immunity and nonlinear incidence satisfying **(P1)**-**(P3)** is a sharp threshold system characterized by its vaccination reproduction number,

$$\begin{cases} \frac{dS}{dt} = \Pi - \alpha S - Sg(I) - \mu S + \omega V, \\ \frac{dV}{dt} = \alpha S + \gamma I + \xi E - (\mu + \omega)V, \\ \frac{dE}{dt} = Sg(I) - (\mu + \sigma + \xi)E, \\ \frac{dI}{dt} = \sigma E - (\mu + \gamma)I. \end{cases} \tag{3.3}$$

4. An application of model (1.2)

Vaccination was the most cost-effective intervention for mitigating the 2010 influenza A(H1N1) pandemic. On 28 August 2009, WHO advised that the countries in the northern hemisphere should prepare for a second wave of pandemic spread [10]. Fortunately, the pH1N1 vaccination programme for five priority groups was launched, such as medical workers, pregnant women, people over 65 or with chronic illness, children aged between 6 months to 6 years [11]. Because the susceptible individuals aged over 6 months were vaccinated with the pH1N1 vaccine instead of newborns and up to 75% of H1N1 infection was asymptomatic due to nature immunity [15], model (1.2) is applied to illustrate that vaccination effectively contained subsequent potential waves of the pandemic (H1N1) 2009 in Hong Kong China in this section.

4.1. Data

At the end of every month from May 2009 to October 2010, the pH1N1 case data of Hong Kong were released by official website of Center for Health Protection, Hong Kong China (available at https://www.chp.gov.hk/sc/statistics/data/10/26/43/416.html [12]), and the data from May 2009 to June 2010 are chosen to fit the parameter values of model (1.2) owing to its high smooth degree (see Fig. 1). Indeed, the prevalence level of from July to October 2010 showed the small fluctuations and kept low (also seeing [8]). The first wave of the pandemic failed to be avoided (see Fig. 1) since there was no available vaccine against the novel influenza strain before 21 December 2009. It was on that day, the pH1N1 vaccination programme for five priority groups was launched and started [11] to minimize any potential second wave and 4182 doses of pH1N1 vaccine were administered [36]. Notice that the vaccine recipients will develop immunity in about 15 days [7] (delayed vaccination, e.g.,[2]), so the start time of generating vaccine-induced immunity can be approximated as 1 January 2010 as shown in Fig. 3 (a).

4.2. Parameter estimation

The intervals or values of parameters and initial condition of model (1.2) are estimated (as shown in Table 1) and explained as follows.
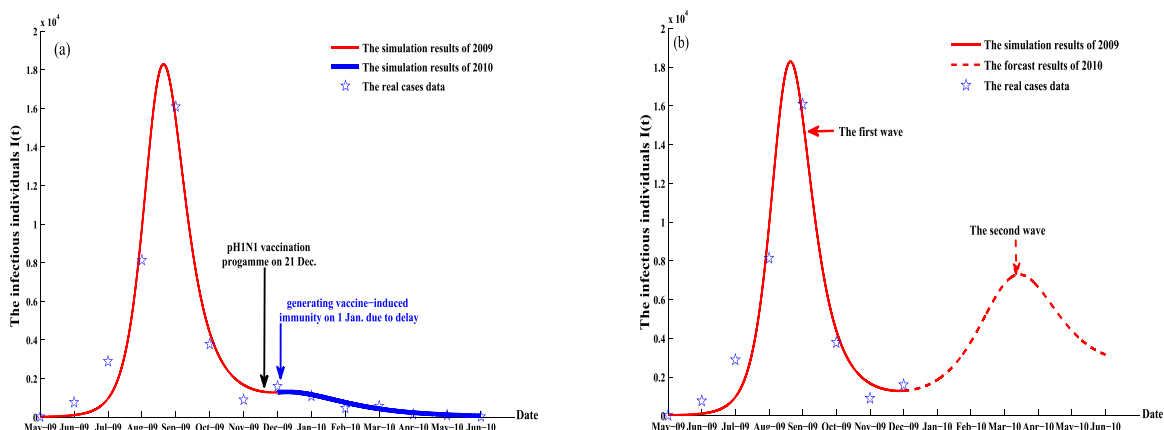
Fig. 3. (a) Comparison of the reported pH1N1 case data in Hong Kong China and the simulated solution $I(t)$ of model (1.2); **(b)** The second wave of the H1N1 pandemic is observed through simulation using the estimated parameter values if the pH1N1 vaccination programme had not been carried out.

Table 2
Model selection for the pH1N1 case data.

Model	AIC	BIC	AICc
$\kappa = 1.3458 \times 10^{-13}$, $q = 0.9287$	113.0446	113.1240	113.7112
$\kappa = 0$, $q = 0.9287$	113.0446	113.1240	113.7112
$\kappa = 0$, $q = 1$	113.8155	113.8950	114.4822

(a) According to Subsection 4.1, we set vaccination rate $\alpha = 0$ during the 2009 pandemic, but α in (0,1] during the 2010 pandemic from [5]. The vaccine effectiveness is up to 99% [37], thus the vaccine is considered to be perfect.

(b) Since life expectancy is about 83.74 years in Hong Kong in 2010 [25], natural death rate $\mu = 30/(83.74 \times 365) = 9.8150 \times 10^{-4}$ per month (m^{-1}).

(c) Following [5,26–28] and [6,7], the infectious duration varies from 4 to 10 days and the immunity period changes in the scope of 180 days to 2 years, respectively, so $1/\gamma \in [4/30, 10/30] = [0.1333, 0.3333]$ and $1/\omega \in [6, 24.3333]$. Let us take the infectious duration and the immunity period as 7 days [27,28] and 1 years [6], respectively, then $1/\gamma = 0.2333$ m and $1/\omega = 12.1655$ m.

(d) The latent period $(1/\sigma)$ ranges from 1 day to 5 days according to Refs[5,26–28]., then $1/\sigma \in [0.0333, 0.1667]$. From [5,26,28], it may be realistic for the influenza A(H1N1) to consider that exposed individuals recover after 1–10 days due to natural immunity, namely, ξ in [3,30]. It is not hard to obtain that the values of parameters q, β and κ belong to [0,1] based on some existing works (e.g., [17,23]).

(e) The number of births of Hong Kong in 2009 [38] was 8.21×10^4 per year, namely, 6748 m^{-1}. Considering that vast majority of newborns were taken protective measures, about 2% of the number of births is chosen as recruitment rate of S class, so $\Pi = 6748 \times 2\% = 130$ m^{-1}. The number of total population of Hong Kong during 2009–2010 [38]) was about 7.0×10^6, thus $N(0) = S(0) + V(0) + E(0) + I(0) \leq 7 \times 10^6$. Together with the case data [12], the initial value $I(0) = 23$ is fixed. And we assume that $E(0) = 10$.

Above all, the values of the remaining parameters β, ξ, σ, q, κ and the initial values $S(0)$, $V(0)$ are estimated (seeing Table 1) with the 8 cases data from May to December 2019 by the DEDiscover simulation tool [39], where we choose the method of Hybrid DESQP Optimization Algorithm, combining global differential evolution and local sequential quadratic programming. From the parameter estimation results above, the values of $\kappa = 1.3458 \times 10^{-13}$, $q = 0.9287$ tend to 0 and 1, respectively. This entails that several standard model selection criteria are employed to evaluate the superiority of models fitting the data [40], including Akaike information criterion (AIC) and Bayesian information criterion (BIC), and their variations such as AICc, with their smaller values corresponding to a better model. It can be observed from Table 2 that model (1.2) with $\kappa = 0$ and $q = 0.9287$ is selected as the best model by the criteria above, and its simulation results are presented in Fig. 3(a). This suggests that the simple mass action incidence βSI may appropriately reflect the short-term transmission process of the emerging influenza A(H1N1) virus and partial temporary immunity should be incorporated into the influenza models. Furthermore, we analyze the error of fitting to evaluate the performances and reliability of model (1.2) with $\kappa = 0$ and $q = 0.9287$, and MAPE (the mean absolute percentage error) and RMSPE (the root mean square percentage error) are computed as MAPE =37.36%, RMSPE =6.76%, respectively. Based on the criteria of MAPE and RMSPE in [41,42], our model can yield reasonable forecasting results. Lastly, from Table 1 it can be checked that the latent period $1/\sigma = 0.1116$ m = 3.3482 days and $1/\xi = 1/(4.2857$ m$^{-1}) = 7$ days are in agreement with the reality.
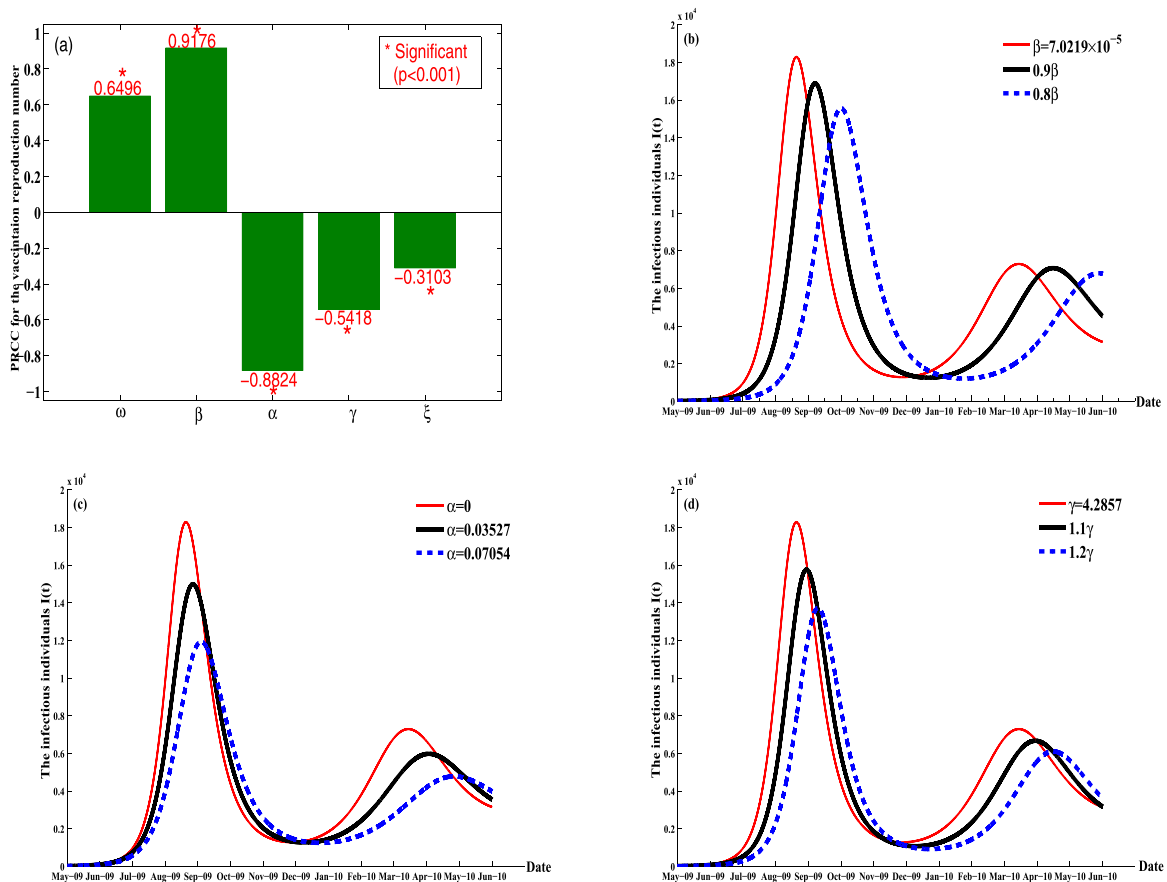
Fig. 4. Sensitivity analysis: **(a)** PRCC values for the vaccination reproduction number $\tilde{\mathfrak{R}}_v$; **(b)** β is decreased by 10%, **(c)** α is increased by 10% and **(d)** γ is increased by 10% of their baseline values in Table 1, respectively.

The results of parameter estimation above yield that the vaccination reproduction number of 2009 is computed into $\tilde{\mathfrak{R}}_v = 1.4675 > 1$, which is consistent with the conclusion in [28,43] (ranging from 1.2 to 2.3). From Theorems 3.4 and 3.5, the disease may be persistent and become endemic. Without vaccination, as forecasted by WHO [10], the second wave is indeed observed through simulation using the estimated parameter values (see Fig. 3(b)), thus vaccination is imperative if the vaccine is available. Furthermore, vaccination rate $\alpha = 0.3527$ is estimated with the case data from January to June 2010 (other parameter values remain the same with Table 1, and initial condition (93492,312020,627,1287) is the simulation result in December 2009, corresponding to $\tilde{\mathfrak{R}}_v = 0.2801 < 1$, such that the pandemic was contained quickly, as proved in Theorem 3.3 and shown in Fig. 3(a).

4.3. Sensitivity analysis

The vaccination reproduction number $\tilde{\mathfrak{R}}_v$ of model (1.2), measuring the average number of secondary cases that are caused when one index case is introduced into a disease-free population [32,33] in which a vaccination programme is carried out, may determine the transmissibility, severity and outcome of the pandemic. In order to seek for effective disease-control measures, we therefore shall be concerned with the effects of input parameters ω, β, α, γ, ξ on $\tilde{\mathfrak{R}}_v$. Based on Latin Hypercube Sampling (LHS) and partial rank correlation coefficients (PRCCs) [44], global uncertainty and sensitivity analysis for $\tilde{\mathfrak{R}}_v$ is conducted to reveal the influence degree on model outcomes. These interesting parameters are considered to obey normal distributions with means coming from baseline values given in Table 1. And their PRCC values are computed through 5000 simulations per run and demonstrated in Fig. 4 (a) and Table 3.

Finally, numerical simulations are carried out to evaluate the effectiveness of disease-control measures. In Table 3, input parameters β, α, ω, γ, ξ are ranked in descending order according to their influences on new infections. In fact, it seems difficult to prolong immunity duration related to the parameter ω. For this reason, we only consider the impacts of parameters β, α and γ. In detail, β has positive impact on $\tilde{\mathfrak{R}}_v$ and α, γ have negative impacts on it. Thus, we decrease the value of β by 10% and increase the value of γ by 10%, respectively. As discussed above, vaccination was such an effective health intervention, that the H1N1 pandemic was successfully curbed in 2010. In consideration of frequent outbreaks of current

Table 3
PRCC values for $\tilde{\mathfrak{R}}_v$, which are ranked from the most sensitive to the least.

Parameter	Mean	Standard deviation	PRCC	p-value
β	7.0219×10^{-5}	2.3406×10^{-5}	0.9176	0
α	0.3527	0.1175	-0.8824	0
ω	0.0822	0.0137	0.6496	0
γ	4.2857	0.4286	-0.5418	0
ξ	4.2857	0.4286	-0.3103	0.1979×10^{-110}

seasonal flu (including influenza A(H1N1), B and C) epidemics in many countries, such as the United States [9] and China with low vaccination rate, it may be interesting and significant to assume that the vaccine is available and vaccination is carried out at the begin of the pandemic. 10% and 20% of vaccination rate $\alpha = 0.3527$ are used to study the effect of vaccination on the pandemic. And the other parameter values and initial values of Table 1 are fixed. Simulation results are presented in Fig. 4 (b)-(d).

Undoubtedly, reducing the disease transmission coefficient β, such as epidemic propaganda, isolation, sterilization and wearing a mask, cuts down the peak of the first wave and delays the arrival of the second wave, but its two peak values fail to decrease obviously even though parameter β is the first sensitive, seeing Fig. 4 (b). On the other hand, increasing vaccination rate α and shortening the disease course of disease γ (e.g., antiviral therapy) lower more dramatically the peak values of the first and second waves than reducing β, but the peak of the second wave arrives much earlier than reducing β (as shown in Fig. 4 (c) and (d)). Therefore, it is possible for policymaker to use multiple control measures jointly during the influenza pandemic. It is also acknowledged that timely vaccination is particularly effective at reducing the outbreak peaks than the other two measures.

5. Conclusion and discussion

Immunization has been bringing mankind great success to prevent the disease transmission every year [2–8,1], and a long latent period of infectious disease may generate dramatically different model prediction and thus allows of no to neglect [26]. What's more, nonlinear incidence can reproduce the inhibition effect from behavioral changes of individuals and the impact of other factors like severity and stage of the infection [16,17,45]. The current work formulates an SVEIS model with vaccination, latency, nonlinear incidence and temporary immunity and establishes its global threshold stability by a novel geometric criterion in [18]. Most pointedly, the open questions on global threshold stability of their EE for two nonlinear SVEIS models with saturated incidence in [16,17] are also well addressed. Inspired by [18], the introduction of the property **(P3)** on the infectious force function $g(I)$ leads us to successfully achieve global threshold dynamics for the SVEIS models with nonmonotone incidence reflecting psychological effect. Furthermore, let $g(I) = \beta I / \varphi(I)$, then an application of Theorem 2.5 yields that model (1.1) is a sharp threshold system provided that $\varphi(I)$ meets $\varphi(0) = 1$ and $0 \leq I\varphi'(I) \leq 2\varphi(I)$, such as $\varphi(I) = 1 + \kappa I^r$ for $0 < r \leq 2$.

In 2009, the novel influenza A(H1N1) virus caused the first pandemic of 21st century. We apply model (1.2) to illuminate the avoidance of the potential second wave of the pandemic (H1N1) 2009 in Hong Kong, China (as predicted by [10]) with the pH1N1 vaccination programme, and it is revealed that timely vaccination is more effective at lowering the outbreak peaks than other measures. This offers solid support for implementation of immunization strategy to cope with current global seasonal influenza burden, measles cases surge and COVID-19 pandemic if the vaccines are available.

This research is also subject to several limitations as follows. In details, observe that HBV vaccine is administered to both newborns and susceptible individuals, so both two vaccination ways can be incorporated into these SVEIS models, which, together with [4] we guess, can still preserve the threshold dynamics since insights provided by several SVEIS models studied above, can inform us that vaccination for either newborns or susceptible individuals and temporary immunity fail to change their threshold stability (see Theorems 2.5, 3.5 and Remark 3.2). Additionally, we just consider the nonlinearity of incidence rate on I, perfect vaccines, constant total population and postulate that vaccine-induced and disease-acquired immunity last the same time. It would be interesting to introduce more general incidence $S^{\varrho}f(I)$ ($\varrho > 0$), distinct vaccinated class (V) and recovered class (R), incomplete vaccination and varying total population size (e.g., [4,18,19,21,45]) to improve the accuracy of model prediction. Certainly, more analytical techniques are needed, and these issues are left as future investigations.

References

[1] WHO, 2020, Immunization coverage, https://www.who.int/news-room/fact-sheets/detail/immunization-coverage, Accessed June 8.

[2] S. Zhao, L. Stone, D. Gao, D. He, Modelling the large-scale yellow fever outbreak in luanda, angola, and the impact of vaccination, PLoS Neglect. Trop. D. 12 (1) (2018) e0006158.

[3] G. Sun, J. Xie, S. Huang, Z. Jin, M. Li, L. Liu, Transmission dynamics of cholera: mathematical modeling and control strategies, Commun. Nonlinear Sci. Numer. Simul. 45 (2017) 235–244.

[4] L. Wang, Z. Liu, X. Zhang, Global dynamics of an SVEIR epidemic model with distributed delay and nonlinear incidence, Appl. Math. Comput. 284 (2016) 47–65.

[5] S. Kim, J. Lee, E. Jung, Mathematical model of transmission dynamics and optimal control strategies for 2009 a/h1n1 influenza in the republic of korea, J. Theor. Biol. 412 (2017) 74–85.

[6] L.A. Grohskopf, D.K. Shay, T.T. Shimabukuro, L.Z. Sokolow, W.A. Keitel, J.S. Bresee, N.J. Cox, Prevention and control of seasonal influenza with vaccines: recommendations of the advisory committee on immunization practices-united states, 2013–2014, MMWR Recomm. Rep. 62 (7) (2013) 1–43.

[7] M. Wang, et al., Antibody dynamics of 2009 influenza a (h1n1) virus in infected patients and vaccinated people in china, PLoS ONE 6 (2) (2011) e16809.

[8] Q. Liao, B.J. Cowling, W.W.T. Lam, R. Fielding, Factors affecting intention to receive and self-reported receipt of 2009 pandemic (h1n1) vaccine in hong kong: a longitudinal study, PLoS ONE 6 (3) (2011) e17713.

[9] Centers for Disease Control and Prevention, Estimated influenza illnesses, medical visits, hospitalizations, and deaths in the United States 2017–2018 influenza season, https://www.cdc.gov/flu/about/burden/estimates.htm. Accessed June 8.2020

[10] WHO, preparing for the second wave: lessons from current outbreaks, 2009. http://www.who.int/csr/disease/swineflu/notes/h1n1_second_wave_20090828/en/. Accessed June 8, 2020.

[11] Department of health hong kong, human swine influenza vaccination programme launched, 2009, http://www.dh.gov.hk/english/press/2009/091221-2.html. Accessed June 8, 2020.

[12] Center for health protection hong kong, number of notifiable infectious diseases by month, 2009, https://www.chp.gov.hk/en/static/24012.html. Accessed June 8, 2020.

[13] E. Metchnikoff, Immunity in Infective Diseases, Binnie, F.G. (transl.), Cambridge University Press, Cambridge, 1905.

[14] T. Ulrichs, Immunity to infectious diseases, in: A. Krämer, M. Kretzschmar, K. Krickeberg (Eds.), Modern infectious disease epidemiology, Springer-Verlag, New York, 2010.

[15] A.C. Hayward, et al., Comparative community burden and severity of seasonal and pandemic influenza: results of the flu watch cohort study, Lancet Respir. Med. 2 (2014) 445–454.

[16] L. Cai, X. Li, Analysis of a SEIV epidemic model with a nonlinear incidence rate, Appl. Math. Model. 33 (2009) 2919–2926.

[17] G.P. Sahu, J. Dhar, Analysis of an SVEIS epidemic model with partial temporary immunity and saturation incidence rate, Appl. Math. Model 36 (2012) 908–923.

[18] G. Lu, Z. Lu, Geometric approach to global asymptotic stability for the SEIRS models in epidemiology, Nonlinear Anal. RWA 36 (2017) 20–43.

[19] G. Lu, Z. Lu, Global asymptotic stability for the SEIRS models with varying total population size, Math. Biosci. 296 (2018) 17–25.

[20] M.Y. Li, J.S. Muldowney, A geometric approach to the global-stability problems, SIAM J. Math. Anal. 27 (1996) 1070–1083.

[21] M.Y. Li, J. Graef, L. Wang, J. Karsai, Global dynamics of a SEIR model with varying total population size, Math. Biosci. 160 (1999) 191–213.

[22] M.Y. Li, J.S. Muldowney, Dynamics of differential equations on invariant manifolds, J. Differ. Equ. 168 (2000) 295–320.

[23] V. Capasso, G. Serio, A generalization of the kermack-mckendrick deterministic epidemic model, Math. Biosci. 42 (1978) 43–61.

[24] D. Xiao, S. Ruan, Global analysis of an epidemic model with a nonlinear incidence rate, Math. Biosci. 208 (2007) 419–429.

[25] U. Nations, Department of economic and social affairs, population division. world population prospects: The 2015 revision, key findings and advance tables, ESA/p/WP.241, 2015.

[26] F. Brauer, P.V.D. Driessche, J. Wu, Lecture Notes in Mathematical Epidemiology, Springer, Berlin, 2008.

[27] A.R. Tuite, et al., Estimated epidemiologic parameters and morbidity associated with pandemic h1n1 influenza, CMAJ 182 (2) (2010) 131–136.

[28] B. Pourbohloul, et al., Initial human transmission dynamics of the pandemic (h1n1) 2009 virus in north america, Influenza Other Resp. 3 (5) (2009) 215–222.

[29] C.J. Briggs, H.C.J. Godfray, The dynamics of insect-pathogen interactions in stage-structured populations, Amer. Nat. 145 (1995) 855–887.

[30] J.A.P. Heesterbeek, J.A.J. Metz, The saturating contact rate in marriage and epidemic models, J. Math. Biol. 31 (1993) 529–539.

[31] P.V.d. Driessche, J. Watmough, Reproduction numbers and sub-threshold endemic equilibria for compartmental models of disease transmission, Math. Biosci. 180 (1) (2002) 29–48.

[32] R. Anderson, R. May, Infectious Diseases of Humans. Dynamics and Control, Oxford Science Publications, Oxford, 1991.

[33] H.W. Hethcote, The mathematics of infectious diseases, SIAM Rev. 42 (4) (2000) 599–653.

[34] T. Li, F. Zhang, H. Liu, Y. Chen, Threshold dynamics of an SIRS model with nonlinear incidence rate and transfer from infectious to susceptible, Appl. Math. Lett. 70 (2017) 52–57.

[35] J.P. LaSalle, The stability of dynamical systems, in: Regional Conference Series in Applied Mathematics, SIAM, Philadephia, 1976.

[36] Department of Health Hong Kong, Statistics on human swine influenza vaccinations, 2009, https://www.dh.gov.hk/english/press/2009/091222.html. Accessed June 8, 2020.

[37] C. Fu, Effectiveness of h1n1 vaccine against reported influenza a(h1n1), Hum. Vacc. 6 (9) (2010) 767–768.

[38] Census and Statistics Department Hong Kong, Press Release: Year-end Population for 2009, https://www.censtatd.gov.hk/press_release/pressReleaseDetail.jsp?charsetID=1&pressRID=2491. Accessed June 8, 2020.

[39] H. Wu, O. Miao, G.R. Warnes, C. Wu, A. LeBlanc, C. Dykes, L.M. Demeter, DEDiscover: a computation and simulation tool for hiv viral fitness research, in: Proceedings of the International Conference on BioMedical Engineering and Informatics, BMEI'08, volume 1, 2008, pp. 687–694.

[40] H. Miao, C. Dykes, L. Demeter, H. Wu, Differential equation modeling of HIV viral fitness experiments: model identification, model selection, and multimodel inference, Biometrics 65 (1) (2009) 292–300.

[41] S.A. DeLurgio, Forecasting Principles and Applications, Tom Casson, New York, 1998.

[42] C.D. Lewis, Industrial and Business Forecasting Methods: A Practical Guide to Exponential Smoothing and Curve Fitting, Butterworths, London, 1982.

[43] P.Y. Boölle, S. Ansart, A. Cori, A.J. Valleron, Transmission parameters of the a/h1n1 (2009) influenza virus pandemic: a review, Influenza Other Resp. 5 (5) (2011) 306–316.

[44] S. Marino, I.B. Hogue, C.J. Ray, D.E. Kirschner, A methodology for performing global uncertainty and sensitivity analysis in systems biology, J. Theoret. Biol. 254 (2008) 178–196.

[45] M. Alexander, S. Moghadas, Bifurcation analysis of an SIRS epidemic model with generalized incidence, SIAM J. Appl. Math. 65 (5) (2005) 1794–1816.